

A Liquid Argon Ionization Chamber Measurement of the Shape of the Beta-Ray Spectrum of K^{40} †

JOHN H. MARSHALL*

Physics Department and Laboratory for Nuclear Science, Massachusetts Institute of Technology, Cambridge, Massachusetts

(Received April 13, 1953)

A liquid argon ionization chamber has been used to compare the shape of the beta-ray spectrum of K^{40} with those of Y^{91} and P^{32} . The K^{40} spectrum is found to be consistent with the shape factor

$$D_2 = p^6 + 7p^4q^2 + 7p^2q^4 + q^6,$$

in agreement with recent measurements.

I. INTRODUCTION

THE shape of the highly forbidden beta-ray spectrum of K^{40} , associated with a spin change of four units, should provide a sensitive test of some of the possible theories of beta decay.¹ However, a milligram of ordinary KCl will emit only one K^{40} beta ray per minute. Using the usual magnetic spectrometer method of measuring beta spectra, it is difficult to obtain sufficient activity to give a counting rate distinguishable from background without making the source so thick that it distorts the beta-ray spectrum. Attempts have been made in recent years to overcome this difficulty,²⁻⁷ both through the use of potassium enriched in K^{40} and by the use of methods which do not require collimation and small source area. The use of an ionization chamber makes possible a large source area and a large solid angle for detection. In principle the energy resolution of an ionization chamber should be better than that of a scintillation spectrometer because thousands of electrons can be collected in every beta-ray pulse giving negligible pulse-height fluctuation due to poor statistics. A liquid argon filling provides a density sufficient to stop the 1.4-Mev beta rays of K^{40} in a chamber of small size and low background. In a liquefied inert gas the electron attachment is low enough to permit electron collection. Using electron collection, it is possible to observe individual beta-ray pulses at counting rates well above background. An investigation of liquid argon ionization chambers of centimeter dimensions is reported elsewhere.⁸

† Assisted by the joint program of the U. S. Office of Naval Research and the U. S. Atomic Energy Commission. The material in this paper comprised part of a Ph.D. dissertation submitted to the Physics Department of Massachusetts Institute of Technology in 1952.

* National Research Council Predoctoral Fellow 1950-1952.

¹ R. E. Marshak, *Phys. Rev.* **70**, 980 (1946).

² Dzelepov, Kopjova, and Vorobjov, *Phys. Rev.* **69**, 538 (1946).

³ D. E. Alburger, *Phys. Rev.* **75**, 1442 (1949).

⁴ Bell, Weaver, and Cassidy, *Phys. Rev.* **77**, 399 (1950).

⁵ D. E. Alburger, *Phys. Rev.* **78**, 629 (1950).

⁶ L. Feldman and C. S. Wu, *Phys. Rev.* **81**, 298 (1951).

⁷ M. L. Good, *Phys. Rev.* **83**, 1054 (1951).

⁸ J. H. Marshall (to be published) and Ph.D. thesis, Massachusetts Institute of Technology, 1952 (unpublished).

II. METHOD

About 17 mg of 110-fold enriched KCl (1.31 percent K^{40})⁹ was placed in a platinum boat and heated in vacuum. The boat was supported from below by long thin electrodes. An aluminum foil cylinder 2 cm in diameter and 12 cm long was slipped over the boat and moved up and down as the KCl evaporated. The KCl deposit near the center of the foil was 0.4 mg/cm² thick and dropped to zero a centimeter from each end. The foil thickness was 1.6 mg/cm². The foil was transferred to the ionization chamber shown in Fig. 1. This chamber was outgassed at about 10 microns pressure at room temperature for 10-20 hours, submerged in a coolant mixture of liquid oxygen and liquid nitrogen at 85-87°K and enclosed by a two-inch thickness of lead. Tank argon¹⁰ at 5 lb/in.² gauge was passed through a trap cooled by liquid oxygen and liquefied directly into the chamber. A negative collecting voltage of 22.5 kv was applied to the foil cylinder. Electron collection pulses with a rise time of about 2 μsec were then observed at anodes 1 and 2. The pulses at anode 1 gave a measure of the beta-ray energy expended inside the foil. The pulses at anode 2 were used to avoid counting beta rays which scattered through the foil.

A schematic diagram of the apparatus is shown in Fig. 2. Los Alamos Model 100 amplifiers were modified to give a 3-μsec rise time and an RC clipping time of 8 μsec. The sweep of an oscilloscope was triggered by pulses from amplifier 1 when they were not accompanied by pulses from amplifier 2. Lengthened pulses from amplifier 1 were applied to the vertical deflection plates of the oscilloscope and photographed on 35 mm film through a vertical slit. The resulting dots were counted with a projector and photomultiplier arrangement that yielded 40 channels for pulse-height analysis. The analyzing system was linear to 1 percent, the channel width constant to within a few percent. Counts due to dirt on the film were negligible. Spurious pulses resulting from the high collecting voltage were eliminated by submerging the voltage supply in oil and by using a long Kovar-glass seal to lead the high voltage

⁹ Supplied by Isotopes Division of Oak Ridge National Laboratory.

¹⁰ Supplied by Air Reduction Company (99.9 percent A, 0.1 percent N₂).

down through the liquid air coolant to the chamber.⁸ The chamber was supported, grounded, and connected to the vacuum system by quarter-inch copper tubing. Microphonics were eliminated by mounting the apparatus on rubber pads. The amplifier connections were made by means of thin wires sealed into glass tubes coated with Aquadag. The input capacity of amplifier 1 (including anode 1, lead, and input grid of 6AK5) was 14 μf . The rms noise level of amplifier 1 was 4.9 μv . Amplifier 2 had an input capacity of about 75 μf and an rms noise of 2.0 μv . The noise levels did not increase noticeably when the high voltage was turned on.

III. PENETRATION EFFECT

The diameter of the rod used as anode 1 was chosen to minimize the dependence of pulse height upon the penetration of a beta ray towards the center of the chamber. In the absence of electron attachment and recombination, a thin wire would normally be used. Most of the pulse would be produced by ionization electrons falling through the steep voltage drop near

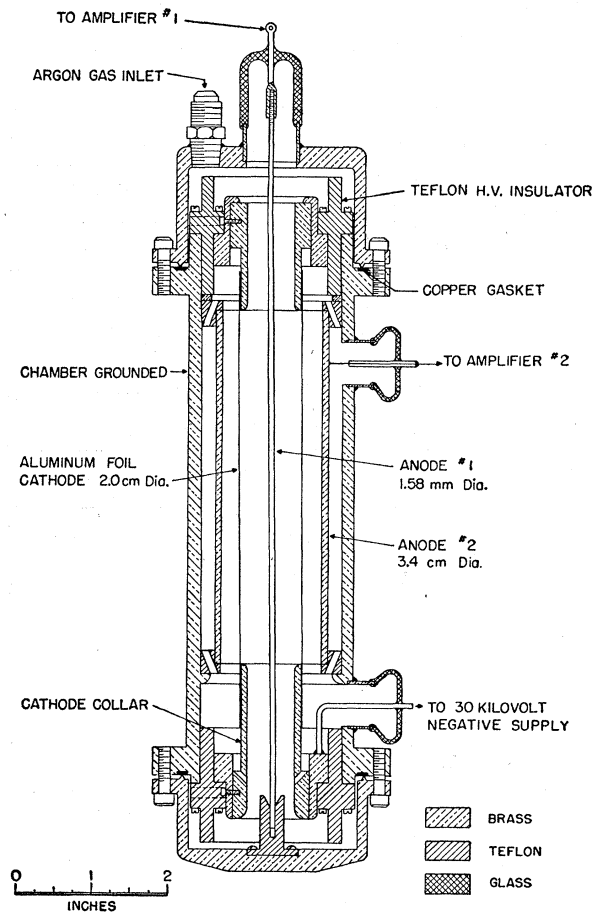


FIG. 1. Cylindrical ionization chamber. The beta-ray source was deposited on the 1.6-mg/cm² aluminum foil cathode. Chamber temperature was 85-87°K. Argon was condensed until liquid argon filled several inches of the filling tube above the chamber.

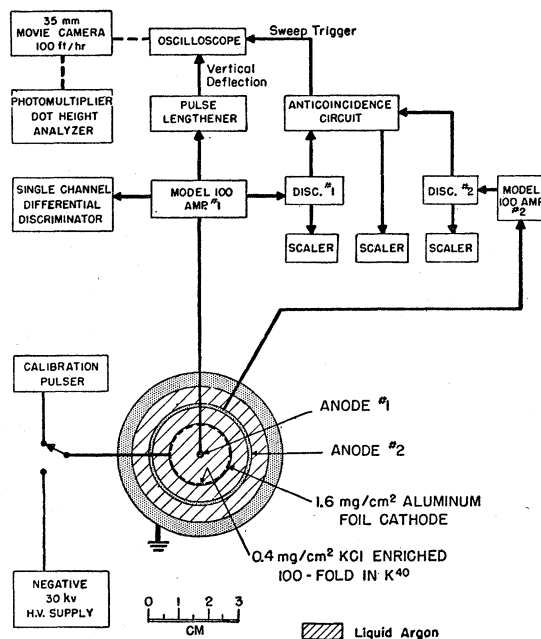


FIG. 2. Apparatus. The beta-ray spectrum was obtained from the pulse-height spectrum from anode 1. Whenever a pulse was also detected at anode 2, the anode 1 pulse was not recorded. Coincidences were caused by beta rays which backscattered from liquid argon through the foil. A top view of the chamber is drawn to scale.

the wire, and pulse height would be practically independent of the radius of the ionizing events. In liquid argon, however, it was found that 5-10 percent of the ionization electrons were lost by attachment to impurity molecules for every millimeter of drift towards the anode. With a thin wire, pulse height would therefore decrease as the radius of ionizing events increased. This would introduce energy nonlinearity and would reduce the energy resolution. Several attempts to reduce the electron attachment by purifying the argon were unsuccessful.⁸

If the anode diameter is increased, the chamber approaches parallel geometry in which pulse height is proportional to the distance the ionization electrons travel. It is possible to balance out geometrical and attachment effects to within a few percent over the outer half of the chamber by using a thick rod as anode. Since the maximum range of 1.4-Mev beta rays in liquid argon is about 4 mm, only the outer half of the (inner) chamber is accessible to betas from the cathode. The thick rod also provides a high enough field in the chamber to reduce recombination to less than 10 percent without the necessity of a higher collecting voltage.

IV. CALIBRATION AND RESOLUTION

The chamber was calibrated using the conversion electrons from the 661-kev level of Cs¹³⁷,¹¹ the beta end

¹¹ L. M. Langer and R. J. Moffat, Phys. Rev. 78, 74 (1950).

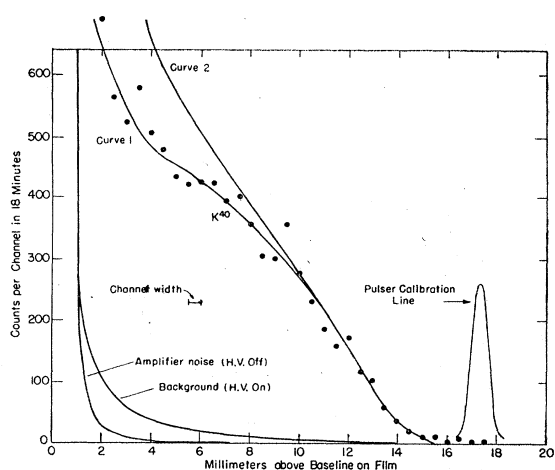


FIG. 3. Typical uncorrected data for K^{40} . The points and curve 1 refer to a discriminator 2 bias for which the minimum detectable energy loss in the outer chamber was 180 kev. Curve 2 refers to a bias of 300 kev. One millimeter on film = 87.5 kev = 16.3 microvolts at anode 1.

point of P^{32} ,¹² and the beta end point of Y^{91} .¹³ The calibration was carried from run to run by comparing the pulses from the internal source with the Compton electron distribution from an external Na^{22} gamma source. This was necessary because the electron collection was not complete but varied between 39 percent and 44 percent for different fillings. This variation in collection was probably caused by a change of less than one part per million in the oxygen introduced into the argon from the walls of the chamber and filling tube. The end-point measurement for K^{40} therefore depended on the Na^{22} comparison and was only accurate to 5–10 percent. Within this accuracy the pulse heights from the chamber were linear with energy. The variation in collection was found not to affect the shape of a spectrum. The K^{40} spectrum measured at 39 percent collection matched that measured in a later run at 44 percent when amplifier gain was changed a corresponding amount.

The position of the Cs^{137} peak corresponded to 120 μ v pulses at anode 1. The full width at half-maximum of the Cs^{137} peak was 100 kev. (The width due to the finite channel and the random noise of amplifier 1 was 70 kev.) The resolution at high energies was not measured. It is possible that the penetration effect described above might by an improper choice of anode diameter increase the width to 150 kev for 1.7-Mev betas.

V. DATA

Figure 3 shows typical uncorrected data for K^{40} . The points and curve 1 were taken with discriminator 2 set so that the minimum detectable pulse in the outer chamber corresponded to an energy of 180 kev. This was the lowest practicable setting and corresponded to

¹² K. Siegbahn, Phys. Rev. **70**, 127 (1946).

¹³ C. S. Wu and L. Feldman, Phys. Rev. **76**, 696 (1949).

the peak noise level of amplifier 2. The curve 1 data give an allowed Fermi plot above 800 kev and an increasing excess of counts at lower energies. (See Fig. 4.)

The dependence of the low-energy excess of counts upon the setting of discriminator 2 shows that at least a large part of the distortion introduced by the chamber is due to beta rays backscattering from the liquid argon through the foil. The coincidence rate (extrapolated to zero bias) indicated that the fraction of the beta rays emitted into one chamber which produced pulses in the other was about 20 percent for P^{32} , 33 percent for Y^{91} , and 26 percent for K^{40} . Incomplete tracks are produced in the inner chamber by beta rays originally emitted outwards as well as inwards. This backscattering has two effects on a spectrum: the low-energy excess of counts which is reduced by anticoincidence, and a deficiency of counts at each energy which is most noticeable at high energies. If the distortion resulting from the first effect is small, a correction factor can be found at each energy for the second effect by measuring the shape of a known spectrum. This empirical correction factor for backscattering deficiency should be independent of the shape of the spectrum because the fraction of beta rays of a given energy which scatter out of the inner chamber is a property of only the liquid argon and the chamber geometry.

Accordingly, thin sources of Y^{91} and P^{32} ($\ll 0.1$ mg/cm²) were evaporated from water solution onto 1.9-mg/cm² aluminum foils and measured in the chamber under conditions similar to those used for K^{40} . Since the source was surrounded by a dense scattering medium, the difference in source thickness is assumed to be unimportant. The probable effect of the combined source and foil thickness is to make the anticoincidence bias 10 to 15 kev higher than the setting of discriminator

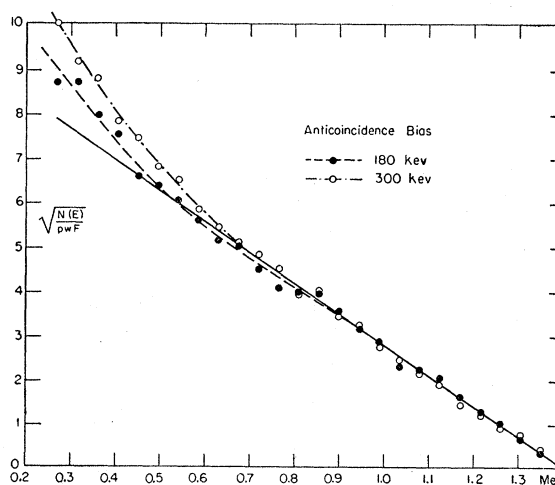


FIG. 4. Fermi plot of K^{40} data. The number of beta rays per unit energy $N(E)$ corrected for background is divided by beta-ray momentum, p , total beta-ray energy W , and the Fermi function F . For F , the Bethe-Bacher approximation was used. The different biases show the effect of backscattering at low energies.

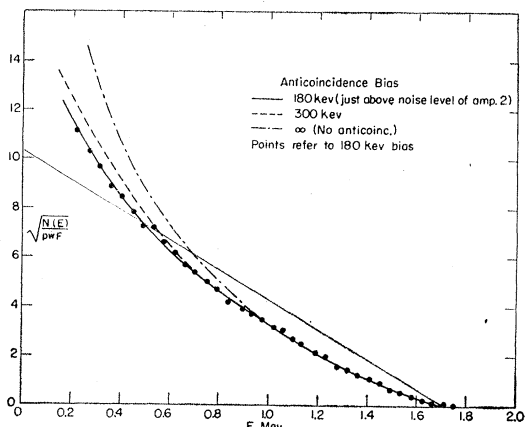


FIG. 5. Fermi plot of P^{32} data. If the chamber introduced no distortion, the P^{32} data would give a straight line. If the low energy excess of counts were negligible (effectively zero bias), the remaining backscattering distortion would be independent of spectral shape and could be corrected empirically.

2. Fermi plots of the data corrected for background are given in Figs. 5 and 6. The P^{32} spectrum is allowed,¹² and if no distortion were present, it would give a straight line plot. The Y^{91} data have been plotted using the first forbidden shape factor,¹³ which would also give a straight line in the absence of distortion. The empirical factor at each energy necessary to linearize the plotted data from P^{32} and Y^{91} was found and applied to Fermi plots of the K^{40} data. No correction has been made for the K^{40} gamma ray since the effect on any point is probably no more than 1 percent.

VI. CONCLUSIONS

The ratio of the corrected K^{40} spectrum to an allowed spectrum is plotted *vs* energy in Fig. 7. The solid curve

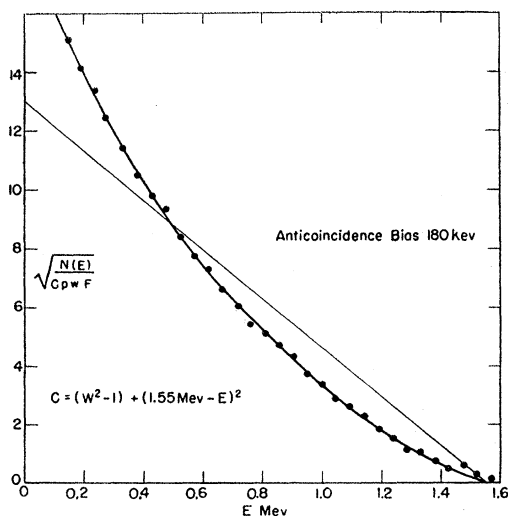


FIG. 6. Fermi plot of Y^{91} data. The first forbidden shape factor $C = (W^2 - 1) + (1.55 \text{ Mev} - E)^2$ should give a straight line plot in the absence of distortion. The Bethe-Bacher approximation was used for F . Screening was neglected.

is the D_2 factor given by Marshak.¹ The data have been normalized at 0.5 Mev. A comparison of the K^{40} spectrum as corrected by P^{32} and that corrected by Y^{91} gives a measure of the accuracy of the method. The K^{40} data are nearer the D_2 curve when corrected by Y^{91} which is closer to K^{40} in shape and end point than is P^{32} . The end point measured for K^{40} is 1.4 ± 0.1 Mev; the error results primarily from the uncertainty in the energy calibration. The effect of end point on D_2 can be seen in Fig. 7.

The difference between the two results can be explained by the fact that the backscattering excess of counts at the normalization point, 0.5 Mev, is not negligible and is greater for K^{40} and Y^{91} than it is for

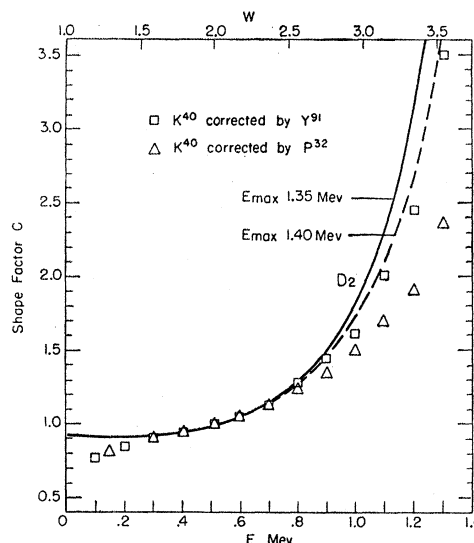


FIG. 7. Comparison of theory and experiment. The K^{40} data for a bias of 180 keV were multiplied by an empirical correction factor found at each energy from Figs. 5 and 6. The ratio of the corrected K^{40} data to an allowed spectrum is plotted *versus* energy. The solid curve is the D_2 shape factor given by Marshak for a K^{40} end point of 1.35 Mev. The dotted curve is D_2 for 1.40 Mev. The K^{40} end point measured from the chamber calibration is 1.4 ± 0.1 Mev.

P^{32} . For this reason the data corrected by Y^{91} should be given greater weight. The difference between the data and the theory below 0.3 Mev is not significant in view of the uncertainty of the backscattering correction. The data agree with the D_2 shape for K^{40} within experimental error in agreement with recent measurements.⁴⁻⁷

$$D_2 = p^6 + 7p^4q^2 + 7p^2q^4 + q^6$$

where p is the beta-ray momentum and q is neutrino momentum.

The D_2 spectrum is given uniquely by the $3T$ and $3A$ interactions and is not inconsistent with $4T$ and $4V$. All four possibilities are compatible with the lifetime of K^{40} .⁶ By the shell model¹⁴ the parity of K^{40} is odd and the parity of its decay product Ca^{40} is even. Since $3T$

¹⁴ L. W. Nordheim, Revs. Modern Phys. 23, 325 (1951).

and $3A$ involve parity change while $4T$ and $4V$ do not, the $K^{40} \rightarrow Ca^{40}$ transition can only be $3T$ or $3A$ (or both). The parity change, the lifetime, and the spin change of four eliminate Fermi interactions from this particular transition. $3T$ and $3A$ are third forbidden Gamow-Teller interactions.

The shape of the beta spectrum of K^{40} is consistent

with the theoretical shape uniquely predicted by beta theory using the known spin change and the parity change given by the shell model. The measured K^{40} spectrum, however, does not seem to eliminate any of the five types of interaction for beta decay in general.

I would like to thank Professor Robley D. Evans for his advice and encouragement throughout this work.

Experimental Evidence for the Fermi Interaction in the β Decay of O^{14} and $C^{10}\dagger$

R. SHERR AND J. B. GERHART
Princeton University, Princeton, New Jersey
(Received April 17, 1953)

The γ -ray spectra of O^{14} and C^{10} have been investigated with a NaI scintillation spectrometer. A value of 2.30 ± 0.03 Mev was found for the O^{14} nuclear γ ray. C^{10} has two γ rays with energies 723 ± 15 and 1033 ± 30 kev; the number of quanta per disintegration are 0.99 ± 0.08 and $1.65 \pm 0.20 \times 10^{-2}$, respectively. The 1033-kev γ ray is associated with a weak positron transition to the 1.74-Mev level in B^{10} . There are less than 10^{-3} transitions per disintegration to the 2.15-Mev level of B^{10} . By combining our results with those of heavy particle reactions and using the predictions of the charge multiplet theory on the energies of the analog states, we conclude that the O^{14} decay and the weak C^{10} branch to the 1.74-Mev level of B^{10} are allowed favored $0 \rightarrow 0$ (no) transitions. From the C^{10} data we find that the ratio of the Fermi to the Gamow-Teller interactions constants (G_F^2/G_{GT}^2) is $0.79_{-0.15}^{+0.27}$, if one assumes $L-S$ coupling, and $0.44_{-0.07}^{+0.15}$ for $j-j$ coupling.

I. INTRODUCTION

IN 1948 some of the main features of the decays of O^{14} and C^{10} were reported.¹ O^{14} was found to disintegrate to an excited state of N^{14} at 2.3 Mev through an allowed positron transition (see Fig. 1). The energy of this excited state corresponded closely to the value calculated for the state in N^{14} which is the $N=Z$ component of the $T=1$ charge multiplet to which the ground states of C^{14} and O^{14} belong. The N^{14*} level at 2.3 Mev appearing in the O^{14} decay was therefore assumed to be this state. (We shall hereafter refer to the charge multiplet state as the analog state.) Since the ground state of C^{14} is known to have spin 0, this identification leads to the interpretation of the $O^{14} - N^{14*}$ decay as a $0 \rightarrow 0$ (no) β transition which requires the Fermi interaction in the theory of β decay. Subsequent to these experiments, the evidence accumulated on the properties of other β transitions seemed to point, with few exceptions, to a satisfactory description of the β decay process in terms of the Gamow-Teller interaction.² Re-examination of O^{14} and C^{10} was undertaken to throw more light on this question.

II. GAMMA RADIATION OF O^{14}

First consideration was given to a better determination of the energy of the 2.3-Mev γ ray in the O^{14} decay, for comparison with the same energy γ ray found in N^{14} in other reactions.^{3,4} A NaI(Tl) scintillation spectrometer was used to compare the photopeak of the 1.28-Mev Na^{22} γ ray with the pair peak of the O^{14} γ ray.⁵ This measurement gave an energy of 2.30 ± 0.03 Mev for the latter γ ray. Thomas and Lauritsen found a 2.310 ± 0.012 -Mev γ ray in the $C^{13}(d, n)N^{14}$ reaction.⁶ The calculation of the energy of the analog state in N^{14} , using recent empirical data, leads to a value of 2.31 Mev.⁷ The close agreement of these numbers constitutes strong support for the identification of the 2.3-Mev level as the analog state in N^{14} .

Recent experimental observations of the reactions $O^{16}(d, \alpha)N^{14}$ ⁸ and $N^{14}(d, d')N^{14}$ ⁹ have been especially interesting because of the absence of α particles and

³ W. F. Hornyak *et al.*, *Revs. Modern Phys.* **22**, 291 (1950).

⁴ F. Ajzenberg and T. Lauritsen, *Revs. Modern Phys.* **24**, 321 (1952).

⁵ W. W. Bell, Senior thesis, Princeton University, 1951 (unpublished).

⁶ R. G. Thomas and T. Lauritsen, *Phys. Rev.* **88**, 969 (1952).

⁷ E. Feenberg and G. Goertzel, *Phys. Rev.* **70**, 597 (1946); E. Feenberg, Nuclear Physics Lecture Notes (unpublished).

⁸ Burrows, Powell, and Rotblat, *Proc. Roy. Soc. (London)* **209**, 478 (1951); A. Ashmore and J. F. Raffle, *Proc. Phys. Soc. (London)* **A64**, 754 (1951); Van de Graaf, Sperduto, Buechner, and Enge, *Phys. Rev.* **86**, 966 (1952).

⁹ Bockelman, Browne, Sperduto, and Buechner, *Phys. Rev.* **90**, 340 (1953); Browne, Bockelman, Buechner, and Sperduto, *Phys. Rev.* **90**, 340 (1953).

[†] A preliminary report of this work was presented at the New York meeting of the American Physical Society January 1952 [*Phys. Rev.* **86**, 619 (1952)]. This work has been supported in part by the U. S. Atomic Energy Commission and the Higgins Scientific Trust Fund.

¹ Sherr, Muether, and White, *Phys. Rev.* **75**, 282 (1949).

² A. Feingold and E. P. Wigner (unpublished communication); C. Wu, *Revs. Modern Phys.* **22**, 386 (1950).